Electronic supplementary information

for

Power generation from nanostructured PbTe-based thermoelectrics: Comprehensive development from materials to modules

Xiaokai Hu,[a,‡] Priyanka Jood,[a,‡] Michihiro Ohta,[a,*] Masaru Kunii,[a] Kazuo Nagase,[a] Hirotaka Nishiate,[a] Mercouri G. Kanatzidis,[b,c], Atsushi Yamamoto[a]

[a]Research Institute for Energy Conservation, National Institute of Advanced Industrial Science and Technology (AIST), Tsukuba, Ibaraki 305-8568, Japan

[b]Department of Chemistry, Northwestern University, Evanston, Illinois 60208, USA

[c]Materials Science Division, Argonne National Laboratory, Argonne, Illinois 60439, USA

‡X.H. and P.J contributed equally to this work.

*Corresponding author: ohta.michihiro@aist.go.jp

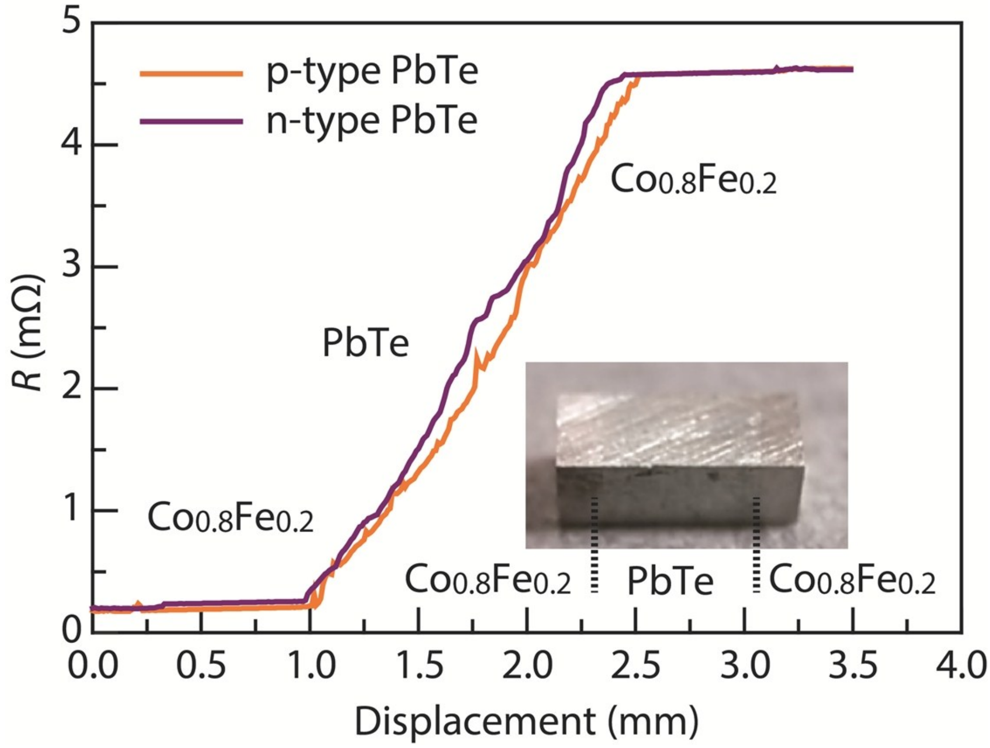

Figure S1

Electrical resistance of PbTe–2% MgTe doped with 4% Na (*p*-type) and PbTe doped with 0.2 % PbI_2 (*n*-type) legs with $Co_{0.8}Fe_{0.2}$ diffusion layers measured by line scanning along the length at room temperature. Few changes have been found for both samples.

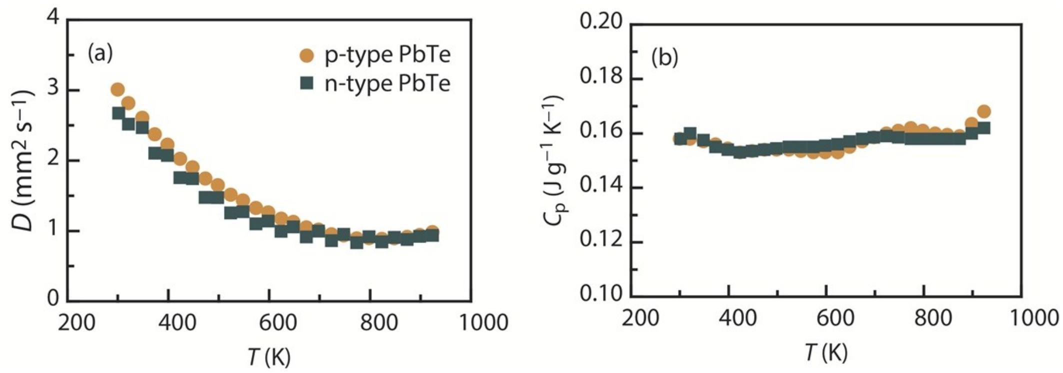

Figure S2

Temperature dependence of the (a) thermal diffusivity (D) and (b) heat capacity (C_P) for the PbTe–2% MgTe doped with 4% Na (p-type) and PbTe doped with 0.2 % PbI_2 (n-type).

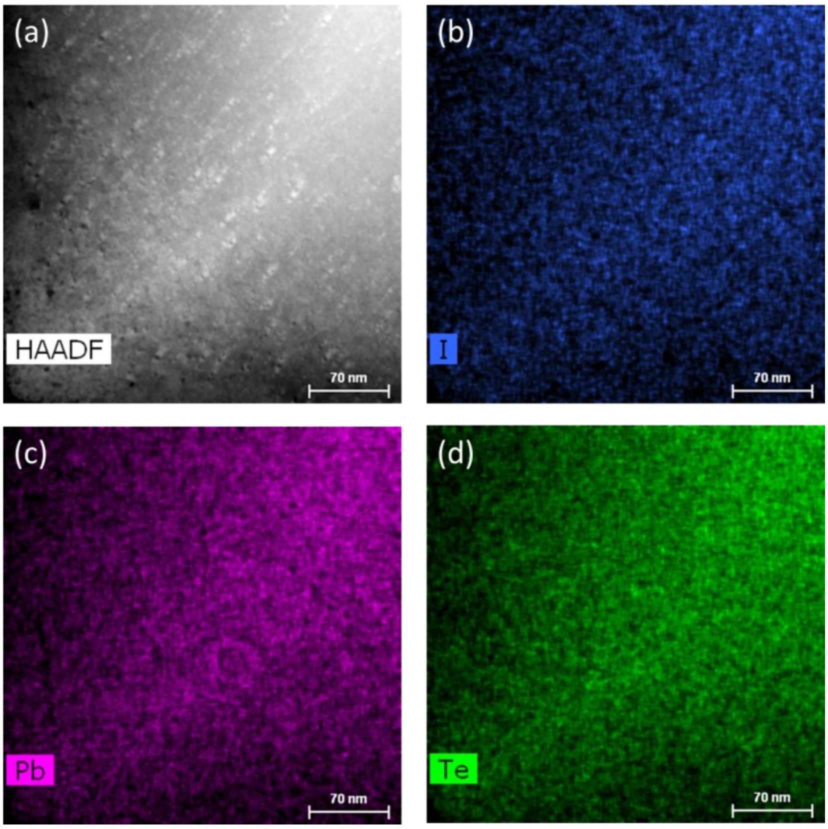

Figure S3

(a) High-angle annular dark-field scanning transmission electron microscope image image of *n*-type PbTe doped with 0.2% PbI_2. (b), (c), and (d) Energy dispersive elemental mapping of the area shown in (a) for elements I, Pb, and Te.

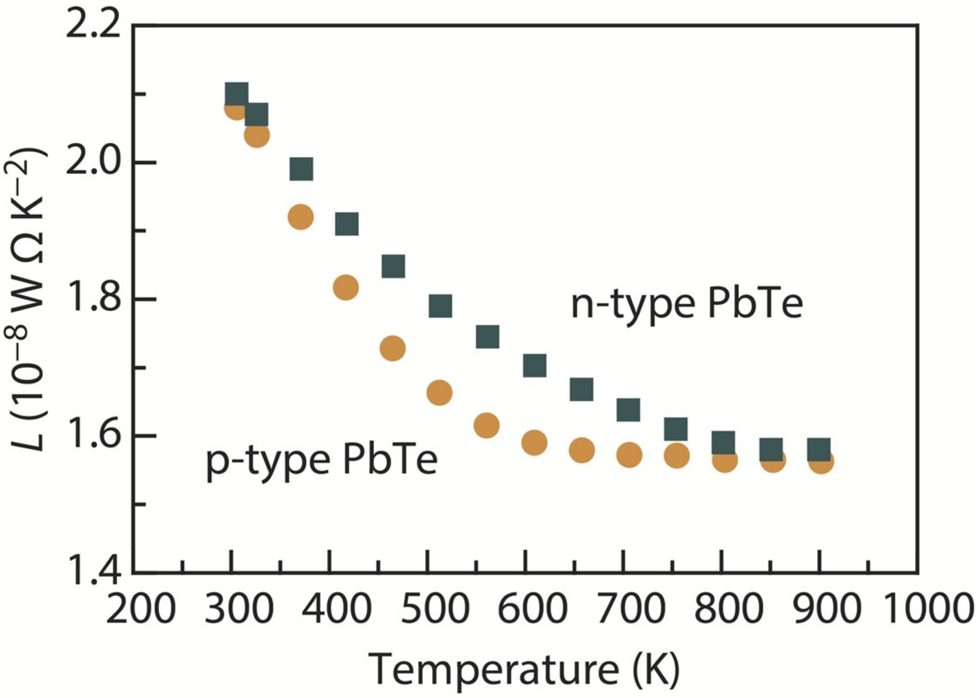

Figure S4

Temperature dependence of the calculated Lorenz number (L) of p-type PbTe–2% MgTe doped with 4% Na and n-type PbTe doped with 0.2% PbI_2.

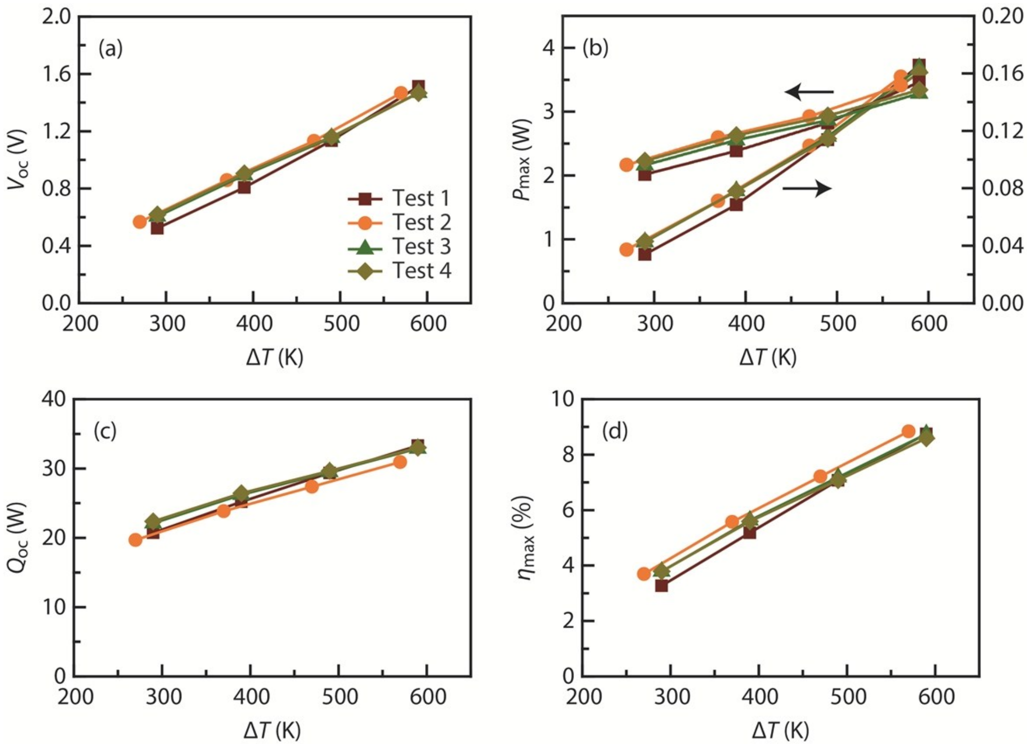

Figure S5

Measured (a) open-circuit voltage (V_{oc}), (b) maximum power output (P_{max}) and internal resistance (R_{in}), (c) open-circuit heat flow (Q_{oc}), and (d) maximum conversion efficiency (η_{max}) of the nanostructured PbTe-based module (PbTe–2% MgTe doped with 4% Na (*p*-type) and PbTe doped with 0.2 % PbI_2 (*n*-type)) as functions of temperature difference (ΔT). The module testing was performed four times on the same module with T_h at 873, 773, 673, and 573 K, and T_c at 283 K except T_c at 303 K for the second measurement to confirm the reproducibility.

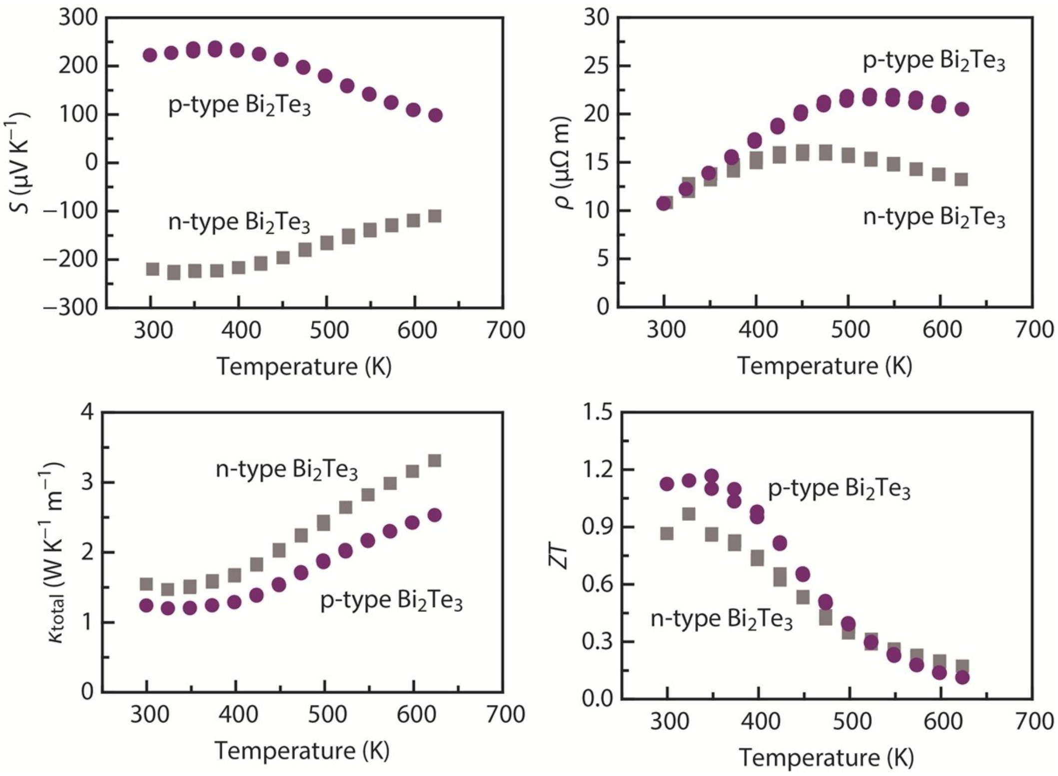

Figure S6

Temperature dependence of the (a) Seebeck coefficient (S), (b) electrical resistivity (ρ), (c) total thermal conductivity (κ_{total}), and thermoelectric figure of merit (ZT) of commercial *p*- and *n*-type Bi_2Te_3 which was used to fabricate the segmented module.

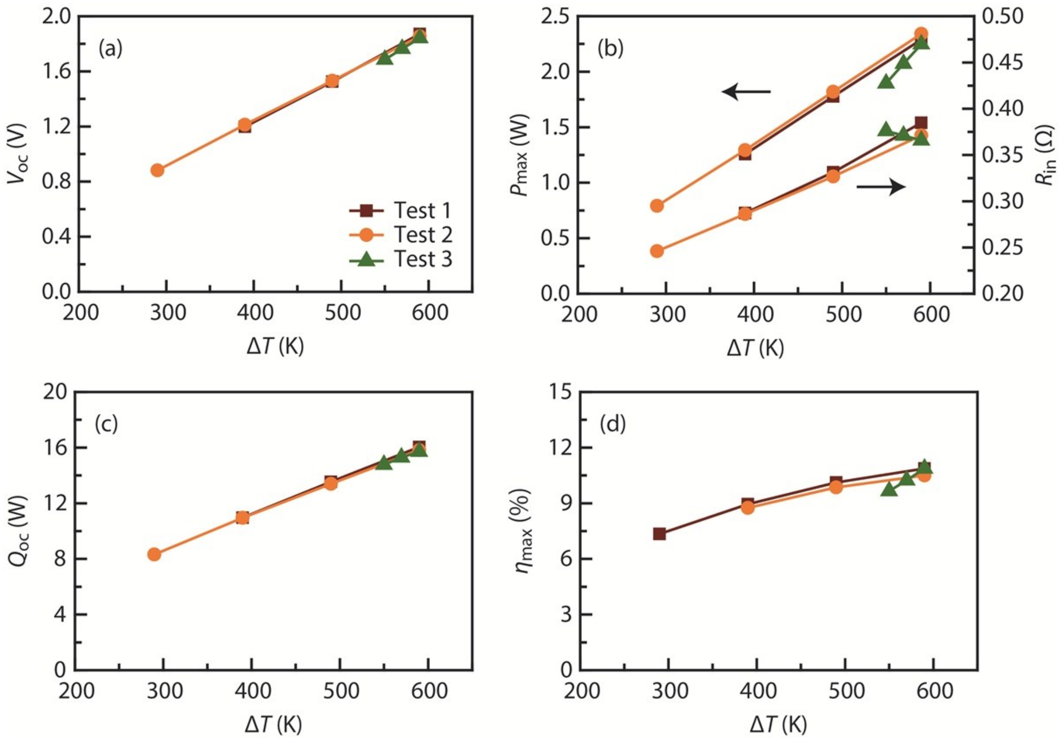

Figure S7

Measured (a) open-circuit voltage (V_{oc}), (b) maximum power output (P_{max}) and internal resistance (R_{in}), (c) open-circuit heat flow (Q_{oc}), and (d) maximum conversion efficiency (η_{max}) of the segmented Bi_2Te_3/nanostructured PbTe (Bi_2Te_3/PbTe–MgTe (*p*-type)–Bi_2Te_3/PbTe (*n*-type)) module as functions of temperature difference (ΔT). The first and second measurements are performed with T_c at 283 K and T_h at 873, 773, 673, and 573 K, while the third measurement is done with T_h at 873 K and T_c at 283, 303, and 323 K.

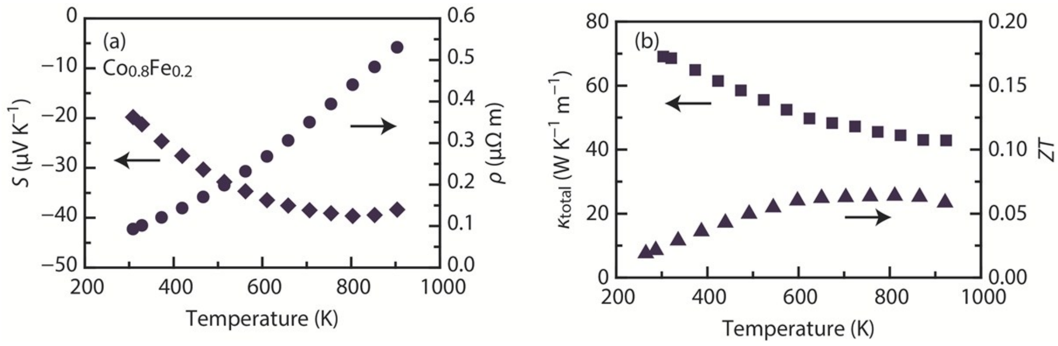

Figure S8

Temperature dependence of the (a) electrical resistivity (ρ) and Seebeck coefficient (S) and (b) total thermal conductivity (κ_{total}) and thermoelectric figure of merit (ZT) of $Co_{0.8}Fe_{0.2}$ which was used as diffusion layer for PbTe legs.

Table S1

Density (*d*) of sintered samples prepared in this study. The theoretical *d* of pure PbTe is 8.24 g cm^{-3}.

Chemical composition	*d* (g cm^{-3})
PbTe–2% MgTe doped with 4% Na	8.08
PbTe doped with 0.2 % PbI_2	7.82

Table S2

Material's properties and geometrical parameters used for simulating power generation of the nanostructured PbTe-based module (PbTe–2% MgTe doped with 4% Na (*p*-type) and PbTe doped with 0.2 % PbI_2 (*n*-type)).

Material	Seebeck coefficient (V/K)	Electrical conductivity (S/m)	Thermal conductivity (W/(m·K))	Size (mm)
p-PbTe-based thermoelectric material	S_p (T) (1)	$1/\rho_p$ (T) (2)	k_p (T) (3)	2×2×2.2
n-PbTe-based thermoelectric material	S_n (T) (1)	$1/\rho_n$ (T) (2)	k_n (T) (3)	2×2×2.2
$Co_{0.8}Fe_{0.2}$ diffusion barrier (Figure S8)	S_{CoFe} (T) (1)	$1/\rho_{CoFe}$ (T) (2)	k_{CoFe} (T) (3)	2×2×0.3
Cu interconnecting electrode	-10^{-6}	8×10^{7}	400	5×2×1 (0.1)
Cu lead wire	-10^{-6}	8×10^{9}	0.01	1×1×4.8
Electrical load resistance	-10^{-6}	10^{-4}, 10^{4}~2×10^{5}	200	1×8×1
Heat sink	NA	NA	200	1×8×0.5
Aluminum substrate	NA	NA	200	18×15×1
Insulated polymer film	NA	NA	10	18×15×0.05

(1)

$S_p(T) = -3.1591\times10^{-13}\,T^3 - 8.1391\times10^{-11}\,T^2 + 7.6928\times10^{-7}\,T - 1.5799\times10^{-4}$

$S_n(T) = 8.8024\times10^{-13}\,T^3 - 1.4263\times10^{-9}\,T^2 + 4.5166\times10^{-7}\,T - 1.1317\times10^{-4}$

$S_{CoFe}(T) = 1.1430\times10^{-16}\,T^3 + 7.9744\times10^{-11}\,T^2 - 1.2843\times10^{-7}\,T + 1.2257\times10^{-5}$

(2)

$\rho_p(T) = -1.5365\times10^{-13}\,T^3 + 2.5123\times10^{-10}\,T^2 - 8.5114\times10^{-8}\,T + 1.1182\times10^{-5}$

$\rho_n(T) = -1.9315\times10^{-14}\,T^3 + 1.2018\times10^{-10}\,T^2 - 7.6049\times10^{-8}\,T + 1.8911\times10^{-5}$

$\rho_{CoFe}(T) = -5.7185\times10^{-16}\,T^3 + 1.5707\times10^{-12}\,T^2 - 4.8920\times10^{-10}\,T + 1.1294\times10^{-7}$

(3)

$k_p(T) = -1.0899\times10^{-8}\,T^3 + 3.0486\times10^{-5}\,T^2 - 2.7721\times10^{-2}\,T + 9.3803\times10^{0}$

$k_n(T) = -1.0776\times10^{-8}\,T^3 + 2.9196\times10^{-5}\,T^2 - 2.5897\times10^{-2}\,T + 8.7124\times10^{0}$

$k_{CoFe}(T) = 1.8876\times10^{-8}\,T^3 + 2.0201\times10^{-5}\,T^2 - 9.0894\times10^{-2}\,T + 9.4741\times10^{1}$